JPP Journal of Pharmacy and Pharmacology

JPP 2007, 59: 645–653

Received July 24, 2006
Accepted February 5, 2007
DOI 10.1211/jpp.59.5.0004
ISSN 0022-3573

Physicochemical characterization of solid dispersions of three antiepileptic drugs prepared by solvent evaporation method

Dionysios Douroumis, Nikolaos Bouropoulos and Alfred Fahr

Abstract

We have investigated the solid dispersion and dissolution profiles of three antiepileptic drugs (carbamazepine (CBZ), oxcarbazepine (OXC) and rufinamide (RFN)) with different aqueous solubilities, prepared by the solvent evaporation method. Solid dispersions of the three drugs in hydroxypropylmethylcellulose (HPMC), with drug:polymer ratios of 1:4, were prepared and characterized by differential scanning calorimetry (DSC), Fourier transformation infrared (FTIR) spectroscopy, X-ray diffraction (XRD) and scanning electron microscopy. The release mechanism was also investigated and the kinetic order of the solid dispersions was evaluated. It appeared that the dissolution behaviour depended on the physicochemical properties of the drug and drug–polymer interactions. DSC thermographs showed amorphous forms for all drugs confirmed by XRD patterns. The FTIR spectra of CBZ and OXC demonstrated drug interactions with HPMC through hydrogen polymer bonds. Thus, solid dispersions of these drugs had an improved dissolution profile. In contrast, solid dispersions of RUF showed modest enhancement of dissolution, suggesting negligible drug–polymer interactions. The different dissolution behaviour is attributed to the extent of interactions between the polymer hydroxyl group and the drug amide groups.

Introduction

Solid dispersions have been widely used to increase the dissolution rate, and hence the bioavailability, of poorly water soluble drugs. They are defined as a dispersion of one or more active ingredients in an inert carrier or matrix in the solid state (Chiou & Riegelman 1971). Solid dispersions are prepared using different techniques, such as solvent evaporation (Hoag et al 2002; Van de Mooter et al 2002; Ohara et al 2005), supercritical methods (Sethia and Squillante 2002, 2004a,b; Jun et al 2005) and hot melt extrusion (Breitenbach et al 1999; Nakamichi et al 2002; Remon et al 2002; Van de Mooter et al 2003; Verreck et al 2005). Usually, a drug substance is incorporated into a water-soluble polymer, leading to a molecular, a crystalline or an amorphous dispersion of the drug. Although the metastable drug form dissolves faster than the crystalline state, the dissolution rate depends on the drug–polymer ratio (Simonelli et al 1976; El-Bana et al 1980; Doherty and York 1987; Sethia & Squillante et al 2002). Polymers have been found to inhibit drug re-crystallization and to affect the physical stability. A number of reports have investigated the principles that govern the enhanced dissolution performance of solid dispersions (Corrigan 1985; Craig 1990; Ford 1986). This behaviour is attributed to reduction of the drug particle size, transformation of the drug to an amorphous state from the crystalline state, the formation of complexes, improved wetting of the drug, and polymer–drug interactions. Several authors have suggested that more than one phenomena contribute to an enhanced dissolution rate.

Carbamazepine (CBZ), oxcarbazepine (OXC) and rufinamide (RUF) are three major antiepileptic drugs classified by the Biopharmaceutics Classification System as class II active pharmaceutical ingredients (Amidon et al 1995, Löbenberg and Amidon 2000; Martinez et al 2002) because they have low water solubility and high intestinal permeability. Both CBZ and OXC are commercially available products (Tegretol and Trileptal, respectively). RUF, a structurally novel compound unrelated to currently marketed antiepileptic drugs, is a broad-spectrum anticonvulsant, which was discovered and developed by Novartis

Phoqus Pharmaceutical Ltd, 10 Kings Hill Avenue, Kings Hill, West Malling, ME19 4PQ, Kent, UK

Dionysios Douroumis

Department of Material Science, Patras, Rio, GR-26000, Greece

Nikolaos Bouropoulos

Department of Pharmaceutical Technology, University of Jena, Lessingstrasse 8, D-07743 Jena, Germany

Alfred Fahr

Correspondence:
Dionysios Douroumis, Phoqus Pharmaceutical Ltd, 10 Kings Hill Avenue, Kings Hill, West Malling, ME19 4PQ, Kent, UK. E-mail: dionysios.douroumis@phoqus.com

Pharma. In Phase III clinical trials completed in the USA and the EU, RUF demonstrated statistically significant efficacy as adjunctive therapy in the treatment of inadequately controlled partial seizures in adults and in seizures associated with Lennox–Gastaut syndrome (Ohtahara 1988; Hrachovy and Frost 1989). The molecular structures of the three drugs are shown in Figure 1.

The dissolution of poorly water soluble drugs is the rate-limiting factor for absorption. It is therefore important to increase the solubility or the dissolution rate in order to enhance absorption and bioavailability.

In the current study we attempted to increase the dissolution rate of three carboxamide derivatives with the same functional groups but different water solubilities, and investigated possible drug–polymer interactions. Few studies have attempted to enhance the dissolution rate of poorly water soluble drugs. This study also attempted to relate the dissolution behaviour to the drug state within the solid dispersions.

Hydroxypropylmethylcellulose (HPMC, Pharmacoat 606) was used as the water-soluble polymer for the solid dispersions, which were produced using solvent evaporation. HPMC has been successfully used for solid dispersions of numerous drugs (Meshali and Gabr 1992; Serajuddin 1999; Ohara et al 2005; Won et al 2005). The HPMC type was selected on the basis of its low viscosity (6 mPa) and the high degree of substitution (DS) of hydroxypopyl and methoxy groups (9% and 29%, respectively). This HPMC type has the highest DS of the aforementioned groups compared with other grades. The assumption was that a high DS could superimpose the drug–polymer interactions. From the effectiveness of HPMC it can be concluded that molecules with a hydrophobic substituent and with hydrated functional groups are useful stabilizers of hydrophobic crystals. As HPMC shows surface activity (Chang and Gray 1978), it can be adsorbed onto the drug surface. In particular, cellulose ethers containing methoxyl or hydroxypropyl groups are adsorbed onto hydrophobic drug surfaces (Rasenack et al 2003). The physicochemical properties of HPMC are strongly affected by the molecular weight and the content of methoxy and hydroxypropyl groups (Siepmann and Peppas 2001).

The physicochemical phenomena affecting the dissolution rate of solid dispersions of different HPMC-containing drugs are not well characterized. There are a few reports in the literature relating to the intra- or intermolecular interactions between the drug and HPMC through hydrogen bonding. The presence or absence of interactions between the drug and polymer molecules has an important effect on the dissolution rate when the drug is in an amorphous state. Another important aspect is the incorporation of polymorphic drugs (CBZ) or ionizable drugs (OXC) in solid dispersions because it can affect the properties of the drug crystals. This affects not only dissolution but also drug stability.

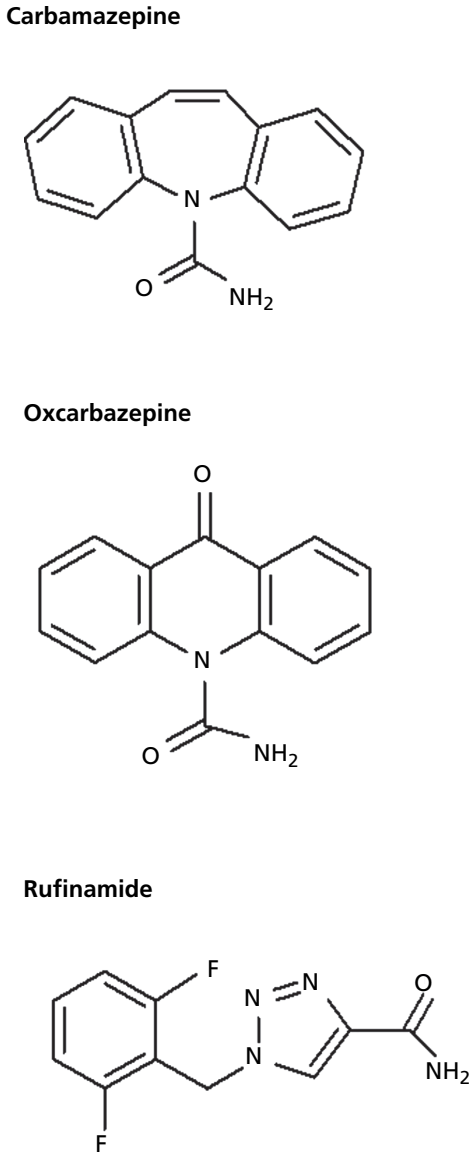

Figure 1 Molecular structures of carbamazepine, oxcarbazepine and rufinamide.

Materials and Methods

Materials

CBZ, OXC and RUF were donated by Novartis Pharma (Basel, Switzerland). Pharmacoat 606 was purchased from Shin-Etsu Chemical Co. (Tokyo, Japan). Tetrahydrofuran, acetonitrile, chloroform and methanol were purchased from Carl Roth (Karlsruhe, Germany). All materials were used as received. Demineralized water was prepared by a high-purity water system (Fa. DEWA, Engineering und Anlagebau GmbH, Vieneburg, Germany).

Preparation of solid dispersions

Solid dispersions of CBZ, OXC and RUF in HPMC were prepared by conventional evaporation methods to produce a drug:polymer ratio of 1:4. The drugs and the polymer were dissolved in minimum chloroform–methanol volumes. In a round-bottomed flask, 0.4 g drug and 1.6 g HPMC were dissolved in 100 mL solvent mixture (chloroform–methanol) (50/50 v/v). A Büchi rotary evaporation system was used to

remove the solvent at 40°C, 460 mbar and 50 rpm. The solid dispersions were ground to a fine powder using a Retsch ball mill (MM 301, Retsch GmbH, Haan, Germany) under liquid nitrogen. The powder produced was passed through a 100 μm sieve and kept in a desiccator until examined.

Differential scanning calorimetry

The physical state of the pure drugs and the solid dispersion samples were examined by differential scanning calorimetry (DSC). The thermograph for each powder was obtained using a Perkin-Elmer Pyris 1 differential scanning calorimeter (Perkin-Elmer Instruments, Norwalk, USA). Accurately weighed samples (2–3 mg) were placed in pierced aluminium pans and heated from 20°C to 240°C at a scanning rate of 10°C min^{-1} in a nitrogen atmosphere.

Powder X-ray diffraction

Samples of pure drugs and drug–polymer dispersions were evaluated using a Philips 1830/40 diffractometer (Karlsruhe, Germany). The samples were radiated using Ni-filtered CuKa radiation operated at 40 kV and 30 mA. The sample was scanned at a diffraction ratio (2θ) from 10 to 40 at a scanning speed of 0.01 $2\theta\, s^{-1}$.

Fourier transformation infrared studies

Fourier transformation infrared (FTIR) spectroscopy was used to investigate intermolecular hydrogen bonding between pure drug and HPMC in solid dispersion products. The technique was performed using the KBr pellet method. Sample powders were mixed with KBr (IR, spectroscopy grade (Merck, Darmstadt, Germany) in a ratio of 1:100. The mixtures were compressed to a 12 mm semitransparent disk by applying a pressure of 8 tonnes for 1 min (Digilab press, Randolph, MA, USA). FTIR spectra over the wavelength range 3800–450 cm^{-1} were recorded using a FTIR spectrometer (Digilab Excalibur, Randolph, MA, USA) at a resolution of 1 cm^{-1}.

Scanning electron microscopy

The morphology of pure drugs and drug–polymer dispersions was examined by scanning electron microscopy (SEM). The samples were attached to aluminium stubs with double-sided adhesive carbon tape then gold coated and examined using a scanning electron microscope (Jeol 5200, Tokyo, Japan).

Dissolution studies

Release of the micronized powders was studied using a USP/Ph. Eur. paddle dissolution apparatus (dissolution tester, Serie DT80, Erweka GmbH, Heusenstamm, Germany). All release studies were carried out under sink conditions in triplicate. The powders were added to 900 mL distilled water at 37°C at a paddle speed of 100 rpm. At predetermined sampling times (2.5, 5, 10, 20, 30, 60, 75, 90, 105 and 120 min), 5 mL aliquots were taken and filtered through a 0.45 μm filter. The removed fluid was immediately replaced with an equal volume of fresh dissolution medium.

Dissolution data analysis

Drug dissolution kinetics were analysed by various mathematical models, which were applied considering the amounts of drug released from 0 to 120 min using SigmaPlot 10.0 software (Systat Software Inc., San Jose, USA) Germany). The models tested are presented in Table 1. GraphPad Instat (GraphPad Software Inc., San Diego, USA) was used to compare the dissolution profiles of the solid dispersions and pure drugs. Comparisons were performed using the Mann–Whitney, non-parametric two-tailed test. The Kruskal–Wallis non-parametric test followed by the Dunn post-hoc multiple comparison test was used to investigate the differences between the three drug–polymer formulations.

HPLC analysis

The concentration of drug in the samples was determined by HPLC. A Beckman Gold system (Fullerton, CA, USA) equipped with a model No. 168 detector at 254 nm and a Macherey–Nagel Nucleosil 100 RP, 5 $\mu \times 3$ mm $\times$ 25 cm column was used for HPLC assay (Düren, Germany). Mobile phase A contained TRIS/EDTA (solution I), acetonitrile and tetrahydrofuran at a ratio of 85:5.5:9.5 v/v/v; mobile phase B contained TRIS/EDTA (solution II), acetonitrile and tetrahydrofuran in a ratio of 20:70.5:9.5 v/v/v. Solutions I and II consisted of 3.63 g TRIS and 186 mg EDTA dissolved in 850 mL or 200 mL demineralized water, respectively. Mobile phases were left to stand for at least 12 h. The flow rate was 0.8 mL min^{-1}. The temperature was elevated to 38°C using a Kontron oven 480 (Kontron Instruments, Rotkreutz, Switzerland). The injection volume was 100 μL. Calibration curves were constructed using standard solutions of known concentrations. The Beckman software calculated the peak area of each standard solution and sample automatically.

Results and discussion

Differential scanning calorimetry

Figure 2 shows representative DSC thermograms of pure CBZ, OXC and RUF and the solid dispersions with HPMC (drug:polymer ratios 1:4). CBZ exhibits enantiotropic polymorphism, which means a transition temperature can be observed below the melting point of either of the polymorphs at which both these forms have the same free energy. Above

Table 1 Dissolution models

Model	Equation
Zero order	$F = k^0 t$
First order	$F = 100\ (1–e^{-kt})$
Higuchi	$F = k_H\sqrt{t}$
Hixson–Crowell	$F = 100\ [1–(1–k_{HC}t)^3]$
Peppas	$F = k_p t^n$

F, amount of drug dissolved in time t, k^0, k_1, k_H, k_{HC}, k_P, dissolution rate constants, n, dissolution exponent.

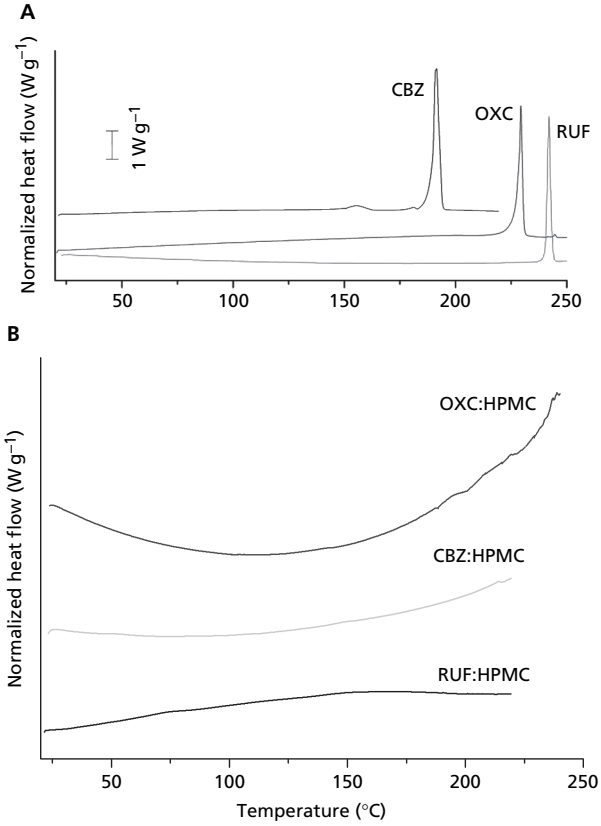

Figure 2 Differential scanning calorimetry curves of pure drugs (A) and solid dispersions in hydroxypropylmethylcellulose (HPMC; 1:4 drug: polymer ratio) (B) of carbamazepine (CBZ), oxcarbazepine (OXC) and rufinamide (RUF). W g^{-1}, is the heat flow mass; all curves were normalized to a sample mass of 1 g.

the transition temperature, the higher melting form (I) has the lower free energy and is more stable. However, the lower melting form III is more stable below the transition temperature since it has lower free energy. The transition temperature of CBZ enantiotropic forms has been reported to be about 71°C (Behme and Brooke, 1991). Hence, under ambient conditions, form III is the more stable form. According to other authors (Lowes et al 1987; Moneghini et al 2001) the DSC thermograms of CBZ samples show two endotherms. The first endotherm is in the range 155–165°C and is not followed by any exothermic event, while a sharp endotherm occurs in the range 189–192°C. This small endothermic peak is characteristic of the transition of the anhydrous monoclinic b-form (form III) to the polymorph I and occurs by solid–solid transformation. Pure CBZ (Figure 2) showed a small melting endotherm at 155.4°C followed by a second endotherm at 191.4°C, which correspond to forms III and I of CBZ, respectively. The melting endotherm at 155.4 °C indicates that the CBZ used herein was form III.

OXC showed a melting endotherm at 229.7°C, where no signs of polymorphism have been observed to date. A water ionization constant (*p*Ka) of 10.7±0.2 has been determined for OXC.

The DSC studies of RUF revealed a melting endothermic peak at 241.9°C.

Pure HPMC showed a glass transition temperature (Tg) at 155°C. Variation in the degree of substitution and the molecular weight plays a role in the observed Tg value. Generally, it has been found that Tg values for HPMC range from 154 to 184°C.

No endothermic peaks corresponding to pure drugs were observed in solid dispersions prepared by the solvent evaporation method. Several studies have shown that HPMC used in solid dispersions can inhibit the crystallization of drugs through formation of an amorphous drug state. Often, drug–polymer interactions through hydrogen bonding can inhibit drug crystallization, particularly in the case of HPMC. The DSC thermographs indicate that all three drugs in the solid dispersions may be present in a completely amorphous or non-crystalline state, due to inhibition of crystallization by HPMC.

Powder X-ray diffraction

XRD was used to investigate the state of the drugs in the solid dispersions produced. Pure forms of the drugs and the drug–HPMC dispersions at 1:4 ratios were also investigated using XRD. The powder XRD patterns of CBZ, OXC, RUF and their solid dispersions are shown in Figure 3. The diffraction spectra of the three drugs show numerous distinct lines of high intensity, indicating that they are in a highly crystalline state. Diffraction peaks for CBZ appeared at 2θ values of 21.9° / 23.4° / 24.0°, 24.9° / 26.7° / 27.3° / 31.9° / 34.9°, for OXC at 13.4° / 17.3° / 18.7° / 19.6° / 20.7° / 22.6° / 25.0° / 25.3° / 25.9° and for RUF at 15.3° / 18.0° / 20.1° / 28.0° / 29.0° / 31.8°.

The powder XRD patterns of the solid dispersions were completely different from those of pure drugs and showed no characteristic peaks. This demonstrates that the drugs were in an amorphous state in the solid dispersions. These results are in agreement with those obtained from the DSC studies. The loss of drug diffraction peaks in all drug–polymer solid dispersions indicates a change in their crystal form during the process.

FTIR spectroscopy

To confirm the presence of hydrogen bonding in the solid dispersions, the FTIR spectra of freshly prepared solid dispersions were compared with those of their corresponding pure drugs and polymer. FTIR is a versatile technique for studying specific interactions between reactive groups in polymer blends as well as between polymer and active substances. Several characteristics, such as the position, form and intensity of spectral bands, provide useful information about the kind and extent of intermolecular forces.

The FTIR spectra for CBZ, HPMC and their solid dispersion complexes are shown in Figure 4. The spectrum of pure HPMC shows a strong band at 1055 cm^{-1}, which is assigned to the C–O–C stretching vibration. The broad band centred at 3480 cm^{-1} corresponds to the –OH stretching vibration and the band at 2939 cm^{-1} is assigned to C–H stretching. The band around 1655 cm^{-1} has been previously assigned to water in the amorphous region (Liang and Marchessault, 1959).

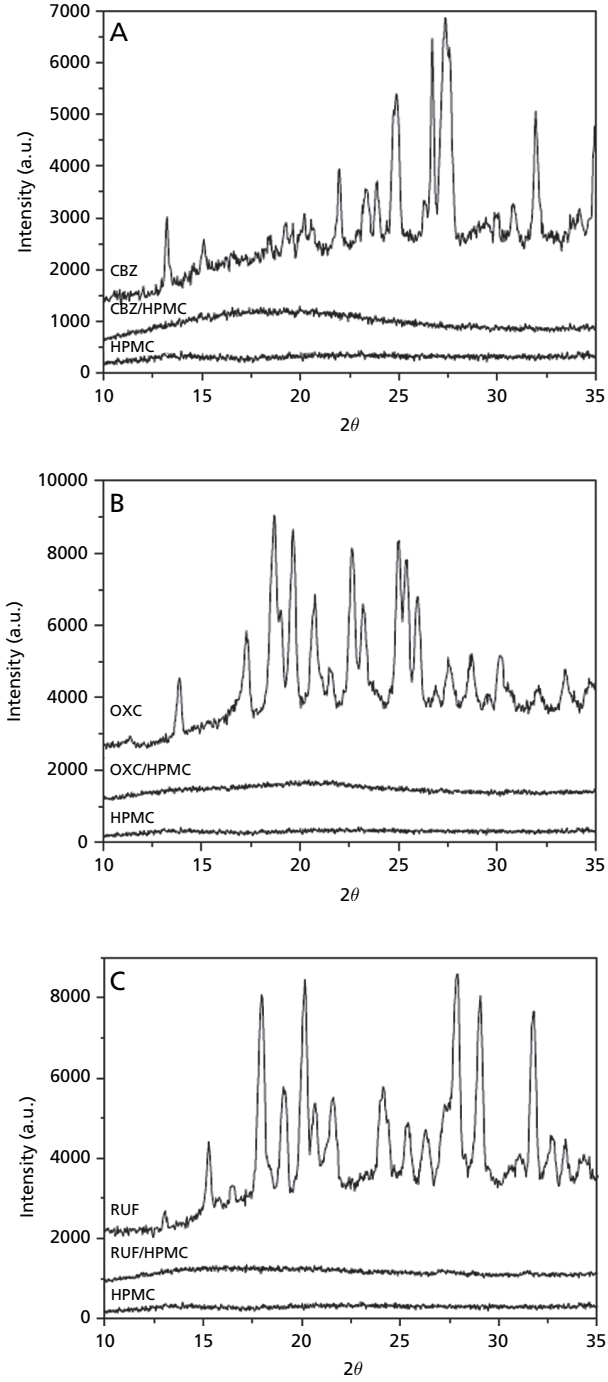

Figure 3 Powder X-ray diffraction patterns for pure drugs and their respective solid dispersion compounds in hydroxypropylmethylcellulose (HPMC) of carbamazepine (CBZ; A), oxcarbazepine (OXC; B) and rufinamide (RUF; C).

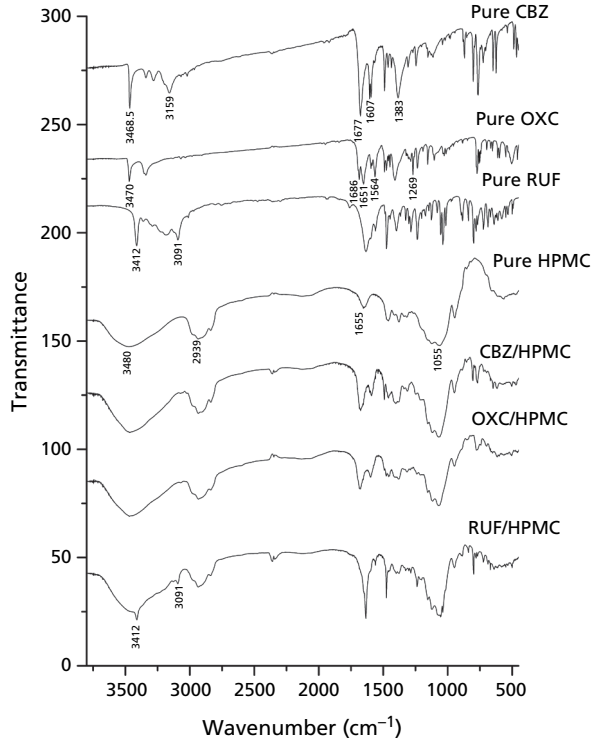

Figure 4 Fourier transformation infrared spectra of pure drugs, hydroxypropylmethylcellulose (HPMC) and solid dispersions (1:4 drug: polymer ratio). CBZ, carbamazepine; OXC, oxcarbazepine; RUF, rufinamide.

The FTIR spectra of CBZ corresponded to those previously reported for form III (Krahn and Mielck, 1987; Lowes et al, 1987; Rustichelli et al, 2000). Characteristic bands of polymorph III were found at 3468.5 cm^{-1} and 3159 cm^{-1} (-NH valence vibration), 1677 cm^{-1} (CO–R vibration), 1607 cm^{-1} and 1594 cm^{-1} (range of –C=C– and –C=O vibration and –NH deformation) and 1383 cm^{-1} (C–NH_2 stretching vibration). The –NH band is located at a lower wave number in polymorph III, and the presence of intermolecular hydrogen bonds should be more marked in this polymorph than in the others.

Substantial differences can be seen in the CBZ–HPMC solid dispersion spectra. The band at 3468.5 cm^{-1} corresponding to the symmetrical N–H stretching vibrations of the primary amide groups of CBZ seen in the pure drug are replaced by a broader band, whereas the 3159 cm^{-1} band, corresponding to the asymmetrical N–H stretching vibrations of primary amide groups, has disappeared. This indicates the possible involvement of –NH_2 groups in hydrogen bonding with the –OH groups of HPMC. In addition, the carbonyl group band is suppressed and is not detectable in solid dispersions spectrum. These results suggest that the N–H and C=O functional groups of CBZ interact with the –OH groups of HPMC at the molecular level in solid dispersions, resulting in extended intermolecular bonding in the amorphous state of CBZ.

In the case of OXC, absorption bands were observed at 3470 cm^{-1} and 3410 cm^{-1} (–NH vibration), 1686 cm^{-1} (–C=O, ketone group vibration), 1651 cm^{-1} (CO–R vibration), 1596 cm^{-1} and 1564 cm^{-1} (range of –C=C– and –C=O vibration and –NH deformation). The spectrum for the OXC solid dispersion shows a broad band in the region of 3200–3500 cm^{-1}, which indicates a chemical interaction of OXC with HPMC via hydrogen bonding in the amorphous state. When such bonds are formed, the compatibility or miscibility between the polymer and the drug increases, changing the spectra, as has been observed in similar studies (Karavas et al 2005).

The FTIR spectra of RUF showed many bands due to triazole and aromatic rings. In addition, the intense bands at 3412 $cm^{-1}$and 3091 cm^{-1} are due to –NH vibration. Figure 4C shows less intensive but distinctive bands at 3412 $cm^{-1}$and 3091 cm^{-1}. If the drug and the polymer interacted, then the functional groups in the FTIR spectra would show band shifts and broadening compared with the spectra for the pure drug and polymer. The FTIR spectra obtained for the RUF solid dispersion showed peaks that were a summation of the characteristic peaks obtained with the pure drug and pure HPMC. This showed that there was no interaction of the drug with HPMC, even in the amorphous state, when the dispersions were prepared using the solvent evaporation method.

In conclusion, the FTIR studies reveal that CBZ and OXC were present as a molecular dispersion within the HPMC carrier, through intermolecular hydrogen bonding, while RUF was present in the amorphous state.

Scanning electron microscopy

SEM images of pure drugs and drugs in solid dispersion complexes are shown in Figure 5. CBZ crystals have a prismatic shape, OXC crystal have a prismatic elongated shape and RUF forms needles-like crystals (Figures 5A, 5B and 5C, respectively). Figures 5D, 5E and 5F show clearly that in the solid dispersion products, the original crystal shape has disappeared and the two components are not detectable. The solid dispersion complexes appear in the form of irregular particles with no homogenicity in size. In addition, it is evident that the solid dispersion complex is significantly smaller than the pure drug.

Dissolution studies

The dissolution profiles of solid dispersions of three poorly water-soluble drugs – CBZ, OXC and RUF – have been

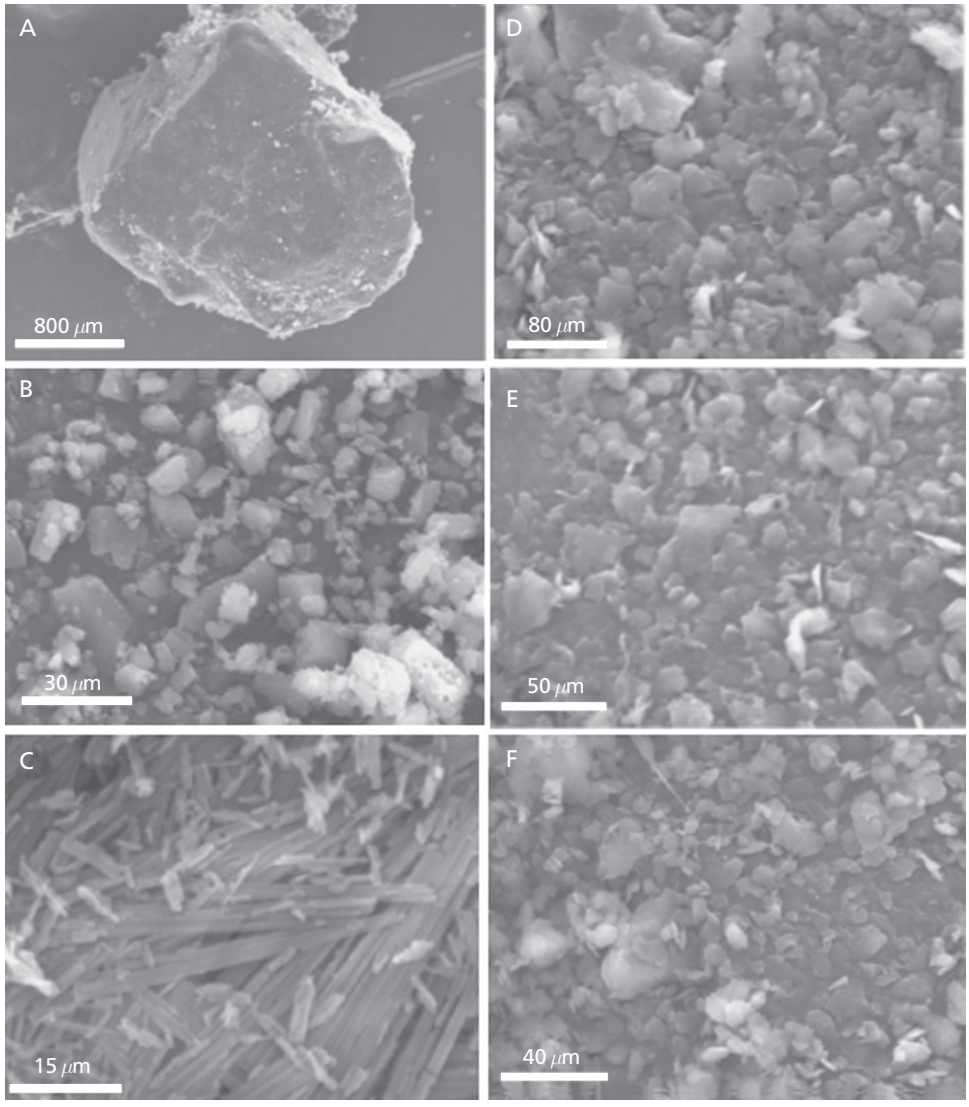

Figure 5 Scanning electron micrographs of pure drugs and hydroxypropylmethylcellulose (HPMC) solid dispersions: carbamazepine (A), oxcarbazepine (B), rufinamide (C), carbamazepine/HPMC (D), oxcarbazepine/HPMC (E), rufinamide/HPMC (F).

investigated. The solubility of these drugs at 25°C is 13, 8.4 and 3.3 mg per 100 mL, respectively, while logP values are 1.76, 1.31 and 7.5, respectively (Stahl 1972). The release profiles of the prepared solid dispersion systems and the pure drugs up to 120 min are presented in Figure 6 and the results are given as percentage (w/w) dissolved as a proportion of the total amount of each sample. Accurately measured weights of the prepared solid dispersions equivalent to 20, 12 and 6.6 mg CBZ, OXC and RUF, respectively, were introduced in 900 mL distilled water to maintain sink conditions ($C < 0.2\,Cs$, where C is the concentration of drug in solution and Cs is the saturation solubility of the drug in equilibrium).

The drug dissolution kinetics from solid dispersions were estimated using the equations presented in Table 1 with the non-linear regression model of SigmaPlot. The parameters calculated by these models and the determination coefficients (R^2) obtained are summarized in Table 2. The fit of each model was predicted depending on these estimations.

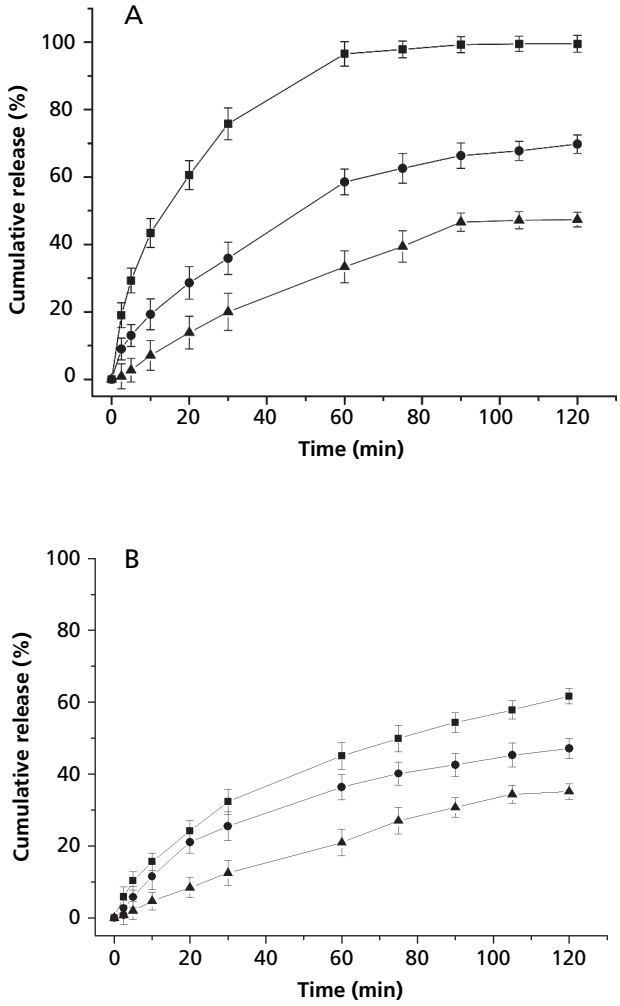

Figure 6 Powder dissolution profiles of carbamazepine (CBZ; ■), oxcarbazepine (OXC; ●) and rufinamide (RUF; ▲) hydroxypropylmethylcellulose solid dispersions (1:4 drug: polymer ratio) in distilled water (A) and pure drugs (B). Data are mean ± s.d. (n = 3).

Considering the R^2 values, the calculated first-order model (Wagner 1969, 1971) successfully fitted CBZ and RUF. The Higuchi model (Higuchi 1961, 1963) fitted OXC but not CBZ or RUF, which indicates that the dissolution kinetics of OXC in solid dispersion may be square-root-time dependent. The zero-order model (Varelas et al 1995) and the Hixson–Crowell model (Hixson and Crowell 1931, Niebergall et al 1963) did not fit all the drug dissolution profiles within the solid dispersions. However, in the case of OXC and RUF, the Peppas model (Siepmann and Peppas 2001) also fitted the dissolution kinetics. Selection of an adequate model was based on comparisons of the following features of each model: higher determination coefficient; smaller standard error of model parameters; and smaller residual mean square (Yuksel et al 2000). On the basis of these comparisons, the Higuchi and first-order kinetic models fit best for OXC and RUF, respectively.

It is well known that, for poorly water-soluble drugs, even a small increase in dissolution could result in a large increase in bioavailability, since the bioavailability of a poorly water-soluble drug is often limited by dissolution rate (Löbenberg and Amidon 2000). The dissolution profiles of the pure drugs and the solid dispersions were therefore compared in order to determine whether a significant difference exists. The P value indicated that the dissolution profiles of RUF and OXC were similar to those of the respective solid dispersions ($P > 0.05$). In contrast, for CBZ there was a significant difference ($P < 0.05$; Mann–Whitney test) between the dissolution profiles of the pure drug and the solid dispersion. Finally, the dissolution profiles of CBZ, OXC and RUF solid dispersions were found to differ significantly ($P = 0.0293$; Kruskal–Wallis test), while the Dunn post-hoc test showed a significant difference only between the RUF and OXC solid dispersion dissolution profiles.

Numerous attempts to improve the dissolution of a drug, and particularly its bioavailability, through solid dispersions have been reported (Simonelli et al 1976; Sekikawa et al 1979; Moneghini et al 2001; Jun et al 2005). Typical mechanisms for the improvement of dissolution characteristics of drugs by solid dispersion are reduction in particle size, the absence of crystallinity due to the formation of amorphous forms, and improved wettability (Leuner & Dressman 2000). Based on the results of our study, the higher dissolution rate of CBZ and OXC solid dispersions could be attributed to the formation of amorphous or non-crystalline forms due to intermolecular hydrogen bonds and molecular adduction, resulting in inhibition of crystallization by HPMC through drug–polymer miscibility, and also increased wettability. The absence of intermolecular hydrogen bonds in RUF solid dispersions was probably the reason for the slight enhancement. Finally, the solid dispersions were stable for at least 6 months, with reproducible dissolution profiles under storage conditions of 25°C and 65% relative humidity.

Conclusions

In the current study, solid dispersions of three antiepileptic drugs were prepared using the solvent evaporation method. The data obtained from DSC, XRD and FTIR studies showed that CBZ and OXC were molecularly dispersed, while RUF

Table 2 Dissolution rate constants and determination coefficients of carbamazepine, oxcarbazepine and rufinamide release from solid dispersions

Dissolution model (see Table 1)		Rufinamide	Carbamazepine	Oxcarbazepine
Zero order	k^0 (% min^{-1})	0.7390 ± 0.1300	0.5709 ± 0.0577	0.4333 ± 0.0300
	R^2	0.7826	0.9158	0.9584
First order	k_1 (min^{-1})	$0.0527 \pm 25 \times 10^{-4}$	$0.0128 \pm 8 \times 10^{-4}$	$0.0063 \pm 2 \times 10^{-4}$
	R^2	0.9911	0.9533	0.9835
Higuchi	k_H (% min^{-1})	10.7543 ± 0.4847	6.7880 ± 0.1355	4.3411 ± 0.2030
	R^2	0.9122	0.9865	0.9451
Hixson–Crowell	k_{HC} ($\%^{1/3}min^{-1}$)	$0.0120 \pm 8 \times 10^{-3}$	$0.0035 \pm 3 \times 10^{-4}$	$0.0019 \pm 7.47 \times 10^{-5}$
	R^2	0.9632	0.9207	0.9745
Peppas	k_P (min^{-n})	20.1121 ± 3.113	6.4875 ± 0.944	1.7221 ± 0.441
	R^2	0.9659	0.9867	0.9836
	n	0.3540 ± 0.0366	0.5105 ± 0.033	0.7126 ± 0.057

k^0, k_1, k_H, k_P, dissolution rate constants, n, dissolution exponent

was in an amorphous state within the solid dispersion. Furthermore, the FTIR spectra of drug–polymer mixtures revealed the formation of intermolecular hydrogen bonding for CBZ and OXC. These interactions were not detected in solid dispersions of RUF, leading to a slight increase in dissolution rate. However, solid dispersions of CBZ and OXC exhibited enhanced dissolution rates, attributed to the intermolecular interactions resulting in inhibition of crystallization and increased wettability.

References

Amidon, G. L., Lunnernas, H., Shah, V. P., Crison, J. R. (1995) A theoretical basis for a biopharmaceutic drug classification: the correlation of in vitro drug product dissolution and in vivo bioavailability. *Pharm. Res*. **12**: 413–420

Behme, R. J., Brooke, D. (1991) Heat of fusion measurement of a low melting polymorph of carbamazepine that undergoes multiple-phase changes during differential scanning calorimetry analysis. *J. Pharm. Sci*. **80**: 986–990

Breitenbach, J., Schrof, W., Neumann, J. (1999) Confocal Raman-spectroscopy: analytical approach to solid dispersions and mapping of drugs. *Pharm. Res*. **16**: 1109–1113

Chang, S. A., Gray, D. G. (1978) The surface tension of aqueous hydroxypropyl cellulose solutions. *J. Colloid Interface Sci*. **67**: 255–265

Chiou, W. L., Riegelman, S. (1971) Pharmaceutical applications of solid dispersion systems. *J. Pharm. Sci*. **60**: 1281–1301

Corrigan, O. I. (1985) Mechanisms of dissolution of fast release solid dispersions. *Drug Dev. Ind. Pharm*. **11**: 697–724

Craig, D. Q. M. (1990) Polyethylene glycols and drug release. *Drug Dev. Ind. Pharm*. **16**: 2501–2526

Doherty, C., York, P. (1987) Mechanisms of dissolution of frusemide–PVP solid dispersions. *Int. J. Pharm*. **34**: 197–205

El-Bana, H. M., El-Gholmy, A. Z., Hammuda, Y. (1980) Phase diagram and dissolution rate studies on hydrochlorothiazide–urea solid dispersions. *Pharm. Acta Helv*. **55**: 244–248

Ford, J. L. (1986) The current status of solid dispersions. *Pharm. Acta Helv*. **61**: 69–88

Higuchi, T. (1961) Rate of release of medicaments from ointment bases containing drugs in suspensions. *J. Pharm. Sci*. **50**: 874–875

Higuchi, T. (1963) Mechanism of sustained-action medication. Theoretical analysis of rate of release of solid drugs dispersed in solid matrices. *J. Pharm. Sci*. **52**: 1145–1149

Hixson, A. W., Crowell, J. H. (1931) Dependence of reaction velocity upon surface and agitation. I. Theoretical consideration. *Ind. Eng. Chem*. **23**: 923–931

Hoag, S. W., Nair, R., Gonen, S. (2002) Influence of polyethylene glycol and povidone on the polymorphic transformation and solubility of carbamazepine. *Int. J. Pharm*. **240**: 11–22

Hrachovy, R. A., Frost, Jr J. D. (1989) Infantile spasms. *Pediatr. Clin. North Am*. **36**: 311–330

Jun, S. W., Kim, M. S., Jo, G. H., Lee, S., Woo, J. S., Park, J. S, Hwang, S. J. (2005) Cefuroxime axetil solid dispersions prepared using solution enhanced dispersion by supercritical fluids. *J. Pharm. Pharmacol*. **57**: 1529–1537

Karavas, E., Ktistis, G., Xenakis, A., Georgarakis, E. (2005) Miscibility behavior and formation mechanism of stabilized felodipine-polyvinylpyrrolidone amorphous solid dispersions. *Drug Dev Ind Pharm* **31**: 473–489

Krahn, F. U., Mielck, J. B. (1987) Relations between several polymorphic forms and the dihydrate of carbamazepine. *Pharm. Acta Helv*. **62**: 247

Leuner, G., Dressman, J. (2000) Improving drug solubility for oral delivery using solid dispersions. *Eur. J. Pharm. Biopharm*. **50**: 47–60

Liang, C. Y., Marchessault, R. H. (1959). Infrared spectra of crystalline polysaccharides. *J Polymer Sci*. **39**: 269–278

Löbenberg, R., Amidon, G. L. (2000) Modern bioavailability, bioequivalence and biopharmaceutics classification system. New scientific approaches to international regulatory standards. *Eur. J. Pharm. Biopharm*. **50**: 3–12

Lowes, M. M. J., Caira, M. R., Lotter, A. P., Van Der Watt, J. G. (1987) Physicochemical properties and X-ray structural studies of the trigonal polymorph of carbamazepine. *J. Pharm. Sci*. **76**: 744–752

Martinez, M., Augsburger, L., Johnston, T., Jones, W. W. (2002) Applying the biopharmaceutics classification system to veterinary pharmaceutical products. Part I. Biopharmaceutics and formulation considerations. *Adv. Drug Deliv. Rev*. **54**: 805–824

Meshali, M. M., Gabr, K. E. (1992) Physical properties of fast-release nonreverting hydrochlorothiazide solid dispersions. *Pharm. Res*. **9**: 960–962

Moneghini, M., Kikic, I., Voinovich, D., Perissutti, B., Filipovic-Grcic, J. (2001) Processing of carbamazepine-PEG 4000 solid dispersions with supercritical carbon dioxide: preparation, characterization, and in vitro dissolution. *Int. J. Pharm*. **222**: 129–138

Nakamichi, K., Nakano, T., Yasuura, H., Izumi, S., Kawashima, Y. (2002) The role of the kneading paddle and the effects of screw revolution speed and water content on the preparation of solid dispersions using a twin-screw extruder. *Int. J. Pharm*. **241**: 203–211

Niebergall, P. J., Milosovich, G., Goyan, J. E., (1963) Dissolution rate studies. II. Dissolution of particles under conditions of rapid agitation. *J. Pharm. Sci*. **52**: 236–241

Ohara, T., Kitamura, S., Kitagawa, T., Terada, K. (2005) Dissolution mechanism of poorly water-soluble drug from extended release solid dispersion system with ethylcellulose and hydroxypropylmethylcellulose. *Int. J. Pharm*. **302**: 95–102

Ohtahara, S. (1988) Lennox–Gastaut syndrome: considerations in its concept and categorization. *Jpn J. Psychiatry Neurol*. **42**: 535–542

Rasenack, N., Müller, B. W., Hartenhauer, H. (2003) Microcrystals for dissolution rate enhancement of poorly water-soluble drugs, *Int. J. Pharm*. **254**: 137–145

Remon, J. P., De Brabander, C., Van Den Mooter, G., Vervaet, C. (2002) Characterization of ibuprofen as a nontraditional plasticizer of ethyl cellulose. *J. Pharm. Sci*. **911**: 678–685

Rustichelli, C., Gamberini, G., Ferioli, V., Gamberini, M. C., Ficarra, R., Tommasini S. (2000) Solid-state study of polymorphic drugs: carbamazepine. *J. Pharm. Biomed. Anal*. **23**: 41–54

Sekikawa, H., Nakano, M., Arita, T. (1979) Dissolution mechanisms of drug-polyvinylpyrrolidone coprecipitates in aqueous solution. *Chem. Pharm. Bull*. **27**: 1223–1230

Serajuddin, A. T. M. (1999) Solid dispersion of poorly water soluble drugs: early promises, subsequent problems, and recent breakthroughs. *J. Pharm. Sci*. **88**: 1058–1066

Sethia, S., Squillante, E. (2002) Physicochemical characterization of solid dispersions of carbamazepine formulated by supercritical carbon dioxide and conventional solvent evaporation method. *J. Pharm. Sci*. **91**: 1948–1957

Sethia, S., Squillante, E. (2004a) In vitro-in vivo evaluation of supercritical processed solid dispersions: permeability and viability assessment in Caco-2 cells. *J. Pharm. Sci*. **93**: 2985–2993

Sethia, S., Squillante, E. (2004b) Solid dispersion of carbamazepine in PVP K30 by conventional solvent evaporation and supercritical methods. *Int. J. Pharm*. **272**: 1–10

Siepmann, J., Peppas, N. A. (2001) Modeling of drug release from delivery systems based on hydroxypropyl methylcellulose (HPMC). *Adv. Drug Deliv. Rev*. **48**: 139–157

Simonelli, A. P., Mehta, S. C., Higuchi, W. I. (1976) Dissolution rates of high energy sulfathiazole-povidone coprecipitates. II: characterization of form of drug controlling its dissolution rate via solubility studies. *J. Pharm. Sci*. **65**: 355–361

Stahl, P. H. (1972) Novartis –Pharmaceutische Entwicklung.

Van den Mooter, G., Verheyen, S., Blaton, N., Kinget, R. (2002) Mechanism of increased dissolution of diazepam and temazepam from polyethylene glycol 6000 solid dispersions. *Int. J. Pharm*. **249**: 45–58

Van den Mooter, G., Six, K., Berghmans, H., Leuner, C., Dressman, J., Van Werde, K., Mullens, J., Benoist, L., Meublat, M. L., Verreck, G., Peeters, J., Brewster, M. (2003) Characterization of solid dispersions of itraconazole and hydroxypropylmethylcellulose prepared by melt extrusion, Part II. *Pharm. Res*. **20**: 1047–1054

Varelas, C. G., Dixon, D. G, Steiner, C. (1995) Zero-order release from biphasic polymer hydrogels. *J. Control. Release* **34**: 185–192

Verreck, G., Decorte, A., Heymans, K, Adriaensen, J, Cleeren, D., Jacobs, A., Liu, D., Tomasko, D, Arien, A., Peeters, J., Rombaut, P., Van den Mooter, G., Brewster, M. E. (2005) The effect of pressurized carbon dioxide as a temporary plasticizer and foaming agent on the hot stage extrusion process and extrudate properties of solid dispersions of itraconazole with PVP-VA 64. *Eur. J. Pharm. Sci*. **26**: 349–358

Wagner, J. G., (1969) Interpretation of percent dissolved-time plots derived form in vitro testing of conventional tablets and capsules. *J. Pharm. Sci*. **58**: 1253–1257

Wagner, J. G., (1971) *Biopharmaceutics and relevant pharmacokinetics*. Drug Intelligence Publications, Hamilton, IL USA, pp 120

Won, D. H., Kim, M. S., Lee, S., Park, J. S., Hwang, S. J. (2005) Improved physicochemical characteristics of felodipine solid dispersion particles by supercritical anti-solvent precipitation process. *Int. J. Pharm*. **301**: 199–208

Yuskel, N., Kanik, A. E., Baykara, T. (2000) Comparison of in vitro dissolution profiles by ANOVA-based, model-dependent and -independent methods. *Int. J. Pharm*. **209**: 56–67